Bai, Chunjiang
Wang, Hui
Ju, Tingting
Shi, Hanwen

COURSE-KEEPING CONTROL FOR DIRECTIONALLY UNSTABLE LARGE TANKERS USING THE MIRROR-MAPPING TECHNIQUE

Summary

This study examines the course-keeping control of directionally unstable large oil tankers involving a pole in the right half plane. Treated as an unstable plant in control engineering, tankers are theoretically and experimentally investigated during the controller design process. First, the unstable plant is mirror-mapped to its corresponding stable minimum phase plant using the mirror-mapping technique, which enables an easy controller design. Then, a linear proportional-differential and a first-order filter controller is designed based on the closed-loop gain shaping algorithm, which requires only one controller parameter to be properly selected based on the system's characteristics. Numerical simulation results confirmed that the designed controller can successfully stabilise an unstable plant subjected to external wind and wave disturbances. The controller designed with the proposed method is suitable for course-keeping control of directionally unstable large tankers. The controller design method is simple with an uncomplicated structure that can easily be implemented in engineering endeavours. Moreover, the rudder motion is small and soft.

Keywords: Course keeping; large tanker; ship motion; directionally unstable

1. Introduction

In the process control industry, multiple plants such as distillation columns, chemical reactors, and bioreactors, become spontaneously unstable. These unstable plants are fundamentally and quantifiably tougher to control compared to stable plants. Considerable attention has been devoted to controlling unstable plants by control engineers after major incidents [1] such as the JAS39 prototype accident on February 2, 1989 and the Chernobyl nuclear power plant accident on April 26, 1986.

Unstable systems exist in oceanic engineering [2], e.g., in the pressure maintenance system of an LNG carrier, the balancing system of an offshore drilling platform and ships under certain circumstances. The instability phenomenon occurs in multiple directions compared to a ship's motion [3]. Furthermore, as modern large tankers are slightly directionally unstable [2], they represent an additional unstable plant in control engineering.

Thus, the motion control of directionally unstable large tankers requires additional theoretical and applied investigations.

In naval architecture, stability has a very wide meaning, thus embracing ship stability fundamentals, ship dynamics, and ultimately ship safety. Ship stability is vitally important for designing and operating ships and other floating structures; moreover, it has been continuously and extensively researched and improved. Bačkalov et al. [4] and Manderbacka et al. [5] extensively reviewed the results at the International Conferences on Stability of Ships and Ocean Vehicles and the International Ship Stability Workshops events during the 2009–2014 and 2015–2017 periods, respectively, thus covering intact and damage stability, regulatory issues such as probabilistic approaches, advanced numerical methods for ship motion, and stability failure prediction such as roll damping, operational issues related to ship stability, and environmental modelling. Applying a simplified analysis method, Yasukawa [6] examined the course stability of a pure car carrier in the proximity of a sloped bank with variable water depth, distance between ship hull and bank, hull drift angle, and heel angle. Numerical simulation results indicated that their analysis method appropriately assesses the course stability of a ship close to a bank. Fitriadhy [7] proposed a numerical model for analysing the course stability of a towed ship in uniform and constant wind. Angelou et al. [8] presented a mathematical model for predicting the behaviour of sailing yachts, as well as analysed the course-keeping instabilities during downwind sailing. By numerically simulating simplified nonlinear mathematical models, Sutulo [9] investigated the dynamic properties of directionally unstable ships during manoeuvring motions. Kim et al. [10] evaluated the manoeuvrability characteristics of the ship sailing in shallow water at low speed by applying the mathematical model considering the shallow water effect. Dlabac et al. [11] confirmed the applicability and efficiency of using PSO method for ship course-keeping optimal autopilot PID controller design. Demirel et al. [12] proposed a fuzzy AHP and ELECTRE method for selecting the most effective roll stabilizing system for a trawler type fishing vessel. Zhang et al. applied the Lyapunov stability method to the stability problem of the control system of underactuated ships undertaking path-following missions [13,14] or dynamic positioning operations [15]. Guan et al. [16] analysed the performances of a quantum neural network steering controller and a conventional proportional-integral-derivative controller in stabilising the course-keeping motion of a ship.

While ship motion stability has been investigated, studies on unstable ship motion control are rarely reported. Neuffer et al. [17] confirmed the global asymptotical stability of a closed-loop system comprising a nonlinear model of a course unstable ship and a proportional derivative (PD) controller. However, their analysis was purely theoretical, based on a one-parameter family of Lyapunov functions, and was not supported by numerical simulations. Gierusz [18] developed a nonlinear model and numerically simulated it on the ship-handling training boat Blue Lady, a very large crude carrier tanker. Their model, which predicts the course of an unstable ship, was confirmed in over 100 experiments in real time. Morawski et al. [19] designed a control system that switches between a turning controller and a course controller to control a ship under different operating conditions. Zhou et al. [20] proposed a nonlinear state-feedback control law for global straight-line tracking control of a course unstable ship but did not consider the influence of wind and waves on the ship's motion. Perera et al. [21] presented a sliding mode controller for the steering system of an unstable ship, which applies partial feedback linearization. Perera et al. [22] proposed a pre-filter-based sliding mode approach that controls the steering system of both stable and unstable ships. However, as the rudder angle is large and the rudder rate is high, the controller parameters are too many to adjust.

Previously, these studies provided in-depth investigations on either stability or control. The course-keeping control of unstable ships in different control modes has progressed.

However, few studies treat a course unstable ship as an unstable plant. Therefore, this area deserves additional theoretical and applied investigations to improve our understanding of the process control and navigation practice.

Consequently, this study develops a concise method for stabilizing an unstable plant such as the course of an unstable ship, especially that of a tanker. A case study is presented for the course-keeping control of directionally unstable large tankers by concurrently adopting the mirror mapping technique (MMT) and the closed-loop gain shaping algorithm (CGSA). Compared with previous studies, the proposed control scheme is of a concise form and involves a simple and fast parameter tuning procedure, thus promoting easy implementation and flexible application relative approaches for unstable large tanker plants.

The remainder of this study is organized as follows. Section 2 introduces the mathematical model of a ship's motion, Section 3 involves a brief description of course stability, and Section 4 comprises an overview of the MMT and CGSA. The proposed control method is presented in Section 5, followed by a large tanker numerical simulation case study in Section 6, and then ends with the conclusion and outlook in Section 7.

2. Mathematical model of ship motion

Considering the plane motion of a ship, the formula simplification method proposed by Abkowitz [23] is adopted hereafter. The hydrodynamic X, Y, N is expanded into a Taylor series form, and only one order form is retained. Considering the left and right symmetry of the ship, the relevant hydrodynamic derivatives such as $X_{\dot{v}}, X_{\dot{r}}, X_v, X_r, X_\delta, Y_{\dot{u}}, Y_u, N_{\dot{u}}, N_u$ are equivalent to zero. Simultaneously, the basic formulas for the ship's motion are linearized on the left side. A linear mathematical model of the ship's plane motion for three degrees of freedom (DOF) can be derived [24] from Equation (1), and then expressed as Equation (2):

$$\begin{cases} m\Delta\dot{u} = X_u\Delta u + X_{\dot{u}}\Delta\dot{u} \\ m\dot{v} + mu_0 r + mx_c\dot{r} = Y_v v + Y_r r + Y_{\dot{v}}\dot{v} + Y_{\dot{r}}\dot{r} + Y_\delta\delta \\ I_{zz}\dot{r} + mx_c\dot{v} + mx_c u_0 r = N_v v + N_r r + N_{\dot{v}}\dot{v} + N_{\dot{r}}\dot{r} + N_\delta\delta \end{cases} \tag{1}$$

$$\begin{bmatrix} m - X_{\dot{u}} & 0 & 0 \\ 0 & m - Y_{\dot{v}} & mx_c - Y_{\dot{r}} \\ 0 & mx_c - N_{\dot{v}} & I_{zz} - N_{\dot{r}} \end{bmatrix} \begin{bmatrix} \Delta\dot{u} \\ \dot{v} \\ \dot{r} \end{bmatrix} = \begin{bmatrix} X_u & 0 & 0 \\ 0 & Y_v & Y_r - mu_0 \\ 0 & N_v & N_r - mx_c u_0 \end{bmatrix} \begin{bmatrix} \Delta u \\ v \\ r \end{bmatrix} + \begin{bmatrix} 0 \\ Y_\delta \\ N_\delta \end{bmatrix}\delta \tag{2}$$

where m is the ship's mass, u is the ship's surge velocity, Δu is the change in surge velocity, v is the ship's sway velocity, r is the ship's yaw rate, δ is the rudder angle, I_{zz} is the ship's mass moment of inertia, x_c is distance from the centre of gravity to the midship, $X_u, X_{\dot{u}}, Y_v, Y_r, Y_{\dot{v}}, Y_{\dot{r}}$ are hydrodynamic derivatives, while $N_v, N_r, N_{\dot{v}}, N_{\dot{r}}$ are hydrodynamic moment derivatives, and Y_δ, N_δ are hydrodynamic derivatives of the rudder force and moment, respectively.

Obviously, the surge velocity u is independent of the sway velocity v and yaw rate r, and can be decoupled, which can be expressed by Equations (3) and (4). After the nondimensionalization of the last two equations, a linear mathematical model of the ship's motion, with a state space form involving two DOFs, can be easily obtained as Equations (5) and (6) where L is the ship's length and V is the ship's velocity. After adding a new state variable, namely, the heading angle ψ, another linear mathematical model of the ship's

motion, in state space form involving three DOF can be properly derived, which can be expressed as Equation (7).

$$m\Delta\dot{u} = X_u\Delta u + X_{\dot{u}}\Delta\dot{u} \tag{3}$$

$$\begin{bmatrix} m - Y_{\dot{v}} & mx_c - Y_{\dot{r}} \\ mx_c - N_{\dot{v}} & I_{zz} - N_{\dot{r}} \end{bmatrix}\begin{bmatrix} \dot{v} \\ \dot{r} \end{bmatrix} = \begin{bmatrix} Y_v & Y_r - mu_0 \\ N_v & N_r - mx_c u_0 \end{bmatrix}\begin{bmatrix} v \\ r \end{bmatrix} + \begin{bmatrix} Y_\delta \\ N_\delta \end{bmatrix}\delta \tag{4}$$

$$\begin{bmatrix} \dot{v} \\ \dot{r} \end{bmatrix} = \begin{bmatrix} a_{11} & a_{12} \\ a_{21} & a_{22} \end{bmatrix}\begin{bmatrix} v \\ r \end{bmatrix} + \begin{bmatrix} b_{11} \\ b_{21} \end{bmatrix}\delta \tag{5}$$

$$\begin{cases} a_{11} = [(I'_{zz} - N'_{\dot{r}})Y'_v - (m'x'_c - Y'_{\dot{r}})N'_v]V / S_1 \\ a_{12} = [(I'_{zz} - N'_{\dot{r}})(Y'_r - m') - (m'x'_c - Y'_{\dot{r}})(N'_r - m'x'_c)]LV / S_1 \\ a_{21} = [-(m'x'_c - N'_{\dot{v}})Y'_v + (m' - Y'_{\dot{v}})N'_v]V / L / S_1 \\ a_{22} = [-(m'x'_c - N'_{\dot{v}})(Y'_r - m') + (m' - Y'_{\dot{v}})(N'_r - m'x'_c)]V / S_1 \\ b_{11} = [(I'_{zz} - N'_{\dot{r}})Y'_\delta - (m'x'_c - Y'_{\dot{r}})N'_\delta]V^2 / S_1 \\ b_{22} = [-(m'x'_c - N'_{\dot{v}})Y'_\delta + (m' - Y'_{\dot{v}})N'_\delta]V^2 / L / S_1 \\ S_1 = [(I'_{zz} - N'_{\dot{r}})(m' - Y'_{\dot{v}}) - (m'x'_c - N'_{\dot{v}})(m'x'_c - Y'_{\dot{r}})]L \end{cases} \tag{6}$$

$$\begin{bmatrix} \dot{v} \\ \dot{r} \\ \dot{\psi} \end{bmatrix} = \begin{bmatrix} a_{11} & a_{12} & 0 \\ a_{21} & a_{22} & 0 \\ 0 & 1 & 0 \end{bmatrix}\begin{bmatrix} v \\ r \\ \psi \end{bmatrix} + \begin{bmatrix} b_{11} \\ b_{21} \\ 0 \end{bmatrix}\delta \tag{7}$$

After the Laplace transformation of the state space mathematical model, the transfer function obtained [2] is shown in Equation (8) as follows:

$$G_{\psi\delta}(s) = \frac{\psi(s)}{\delta(s)} = \frac{K(1+T_3 s)}{s(1+T_1 s)(1+T_2 s)} \tag{8}$$

where s is the Laplace operator, ψ is the heading angle, and K and T_i (i=1, 2, 3) are the maneuverability indices of the ship.

After reducing the order of the transfer function to the second order, the famous Nomoto model is obtained [2] and represented by Equation (9) as follows:

$$G_{\psi\delta}(s) = \frac{\psi(s)}{\delta(s)} = \frac{K}{s(1+Ts)} \tag{9}$$

where $T = T_1 + T_2 - T_3$. For a directionally stable ship, T is positive, whereas it is negative for a directionally unstable ship.

Considering a 389100-ton unstable large tanker [2] as an example in this study, the ship's parameters are presented in Table 1.

Table 1 Parameters of an unstable tanker[2]

L(m)	V(m/s)	▽(dwt)	K	T₁	T₂	T₃
350	8.1	389100	−0.019	−124.1	16.4	46.0

The second-order Nomoto model is represented by Equation (10), which obviously highlights an unstable pole in the right half plane.

$$G_{\psi\delta}(s) = \frac{0.019}{s(153.7s-1)}$$

(10)

3. Course stability

Straight-line stability can be considered as the most important and basic characteristic of a ship. An uncontrolled marine vessel moving in a straight-line path is referred as dynamically straight-line stable when it can spontaneously return to a new straight-line path subsequent to disturbance in the yaw motion direction without considering any corrective rudder actions. Consequently, straight-line instability refers to the case where the ship enters a starboard or port turn subsequent to being disturbed in the yaw motion direction without any rudder deflections. A ship lacks course stability when straight-line stability is absent. The ship's straight-line motion can be guaranteed if the Nomoto time constant T is positive and vice versa.

Most modern large tankers are slightly unstable [2], with common negative Nomoto time constant T. Furthermore, if a ship produces a negative Nomoto gain constant K, the ship exhibits a reverse response phenomenon for the rudder deflection and yaw direction, which represents a form of ship instability. In navigation practice, unstable ships such as large tankers sometimes exist in this unique state. Moreover, the Nomoto model for unstable large tankers can be recognized as an unstable plant in control engineering.

4. CGSA and MMT

4.1 Closed-loop gain shaping algorithm (CGSA)

CGSA for a single input and single output (SISO) system is adopted in this study, with a sketch of the unit feedback control shown in Figure 1. $C(s)$ and $G(s)$ are the controller and the controlled plant, respectively. The variables r, e, u, d_1, d_2, and y correspond to the reference, the error, the control input, the load disturbance, the output disturbance, and the system output, respectively.
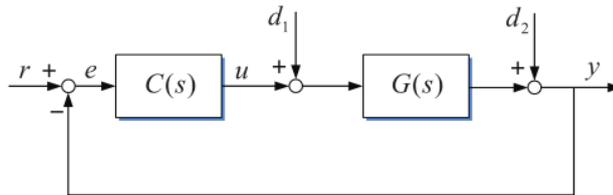
Fig. 1 Diagrammatic sketch of the unit feedback control

CGSA is a simplified $H\infty$ mixed sensitivity algorithm by directly shaping the singular value curves of the sensitivity function $S(S = 1 / (1 + GC))$ and the complementary sensitivity function T ($T = GC / (1 + GC)$), as shown in Figure 2, with the correlativity $T = I - S$ existing between S and T, wherein I is a unit matrix. According to $H\infty$ robust control theory, the closed-loop frequency spectrum, which is equivalent to the T of a typical control system such as that in Figure 1, involves low-pass characteristics to guarantee robust performance of the system. The largest singular value equals 1 such that the system can follow the reference signal without tracking error. In Figure 2, the control performance is favourable if the bandwidth frequency of the closed-loop system (i.e., the crossover frequency $1/T_0$, where T_0 is usually the reciprocal of bandwidth frequency) is appropriately selected. The high-frequency

asymptote slope of T can determine the sensitivity of the system to an invalid disturbance frequency.
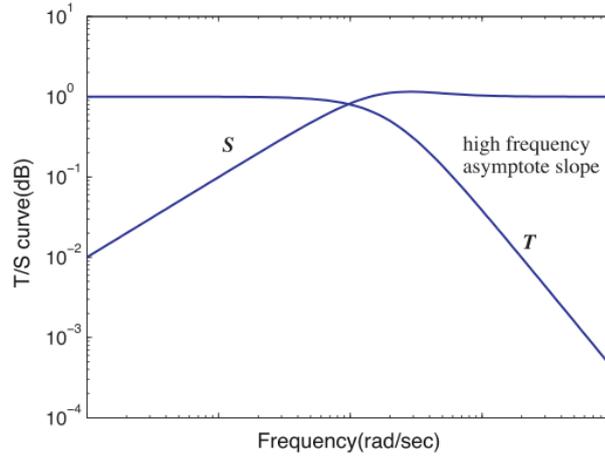
Fig. 2 Typical S and T singular value curves[25]

For common stable plant $G(s)$ in the unit feedback block diagram of Figure 1, the high-frequency asymptotic slope of $T(s)$ in Figure 2 is usually suggested as −20 dB/dec, −40 dB/dec and −60 dB/dec, corresponding to the selection $T(s) = 1 / (T_0 s + 1)^n$ with n = 1, 2 and 3, respectively. Then, the control law $C(s)$ can be derived by Equation (11), namely, the so-called CGSA. The selection of the order number n depends on the relative order number of the controlled plant to achieve the required control law.

$$T(s) = \frac{1}{(T_0 s + 1)^n} = \frac{C(s)G(s)}{1 + C(s)G(s)}, n = 1, 2, 3, \ldots$$

$$\Rightarrow$$

$$C(s) = \frac{1}{G(s)(C_n^0 T_0^n s^n + C_n^1 T_0^{n-1} s^{n-1} + \cdots + C_n^{n-1} T_0 s)}$$

$$C_n^i = \frac{n!}{(n-i)! \cdot i!}, n = 0, 1, \ldots, n-1$$

$$(11)$$

The parameter C_n^i is the binomial coefficient of the binomial expression of $(T_0 s + 1)^n$.

Moreover, CGSA can be applied for the multiple input multiple output (MIMO) and non-square systems, and additional details are available in [26-28].

4.2   Mirror mapping technique (MMT)

The MMT is based on definitions 1 and 2.

Definition 1. For an unstable plant, the mirror-images of the unstable plant refer to the symmetric values (finally lie in the open left half plane) of the zeros or poles that are located in the open right half plane.

Definition 2. For an unstable plant, the mirror mapping process is a process wherein zeros or poles are substituted with their mirror-images for obtaining the minimum phase plant of similar form to the unstable plant.

To explain the MMT, we consider an unstable plant $G(s)$ involving a zero z_0 and a pole p_0 in the open right-half plane as an example. This plant is expressed by Equation (12). The stable minimum-phase plant $G_m(s)$ can then be obtained by MMT after symmetrizing the zero

z_0 and pole p_0 to the open left-half plane with the imaginary axis as the symmetry axis, expressed as Equation (13).

$$G(s) = \frac{s-z_0}{s-p_0}$$ (12)

$$G_m(s) = \frac{s+z_0}{s+p_0}$$ (13)

Note that the largest singular value curve of the minimum-phase plant obtained using the mirror mapping process is similar to the largest singular value curve of the unstable plant; however, the peak value corresponding to the corner frequency might marginally differ between the unstable and stable plants in certain special cases. Furthermore, the unstable plant can be successfully stabilized by the controller that stabilizes the minimum phase plant.

Note that MMT has been successfully adopted in the control of unstable systems with dual pole and dual zero [29], integration of unstable delay processes [25], high-order unstable processes with time delay [30], and industrial unstable processes [31]. Moreover, it is validated in systems such as pure unstable delay systems [32], the pressure maintenance systems of LNG carriers [27, 33], and the Maglev train. The mirror mapping process will be presented in Section 5.

5. Controller design

5.1 Controller design process

This section discusses the course keeping for unstable large tankers in which both the Nomoto time constant T and the Nomoto gain constant K are negative. By ensuring proper rudder action, the tanker will certainly sail along the setting course. Moreover, the global asymptotical stability of unstable ship dynamics utilizing PD control has been proven in the literature [17] using a one-parameter family of Lyapunov functions. This study describes an appropriate and simple PD controller design method. The controller, which is suitable for stabilizing unstable plants such as unstable large tankers, is designed using MMT and CGSA. First, the unstable plant is transformed into an appropriate form that is more convenient for the MMT, as shown in Equation (14). This form considers the sign of the Nomoto time constant T and the Nomoto gain constant K.

$$G(s) = \frac{K}{s(Ts+1)} = \frac{-|K|}{s(-|T|s+1)} = \frac{|K|}{s(|T|s-1)}$$ (14)

Obviously, there is an unstable pole $s = \dfrac{1}{|T|}$ in the right half plane. Then, the unstable plant can be mirror-mapped into its corresponding minimum phase plant based on the MMT as shown in Equation (15) wherein $G_m(s)$ is the minimum phase plant.

$$G_m(s) = \frac{|K|}{s(|T|s+1)}$$ (15)

Applying second order CGSA, wherein the order number n equals to 2 in Equation (11), the second order CGSA controller can be easily obtained for the unstable plant of course

unstable large tankers, as shown in Equation (16), which is equivalent to a linear proportional-differential (LPD) and a first-order filter controller.

$$C(s) = \frac{|T|s+1}{|K|(T_0^2 s + 2T_0)} = \frac{1}{T_0 s + 2} \cdot \left(\frac{|T|s}{|K|T_0} + \frac{1}{|K|T_0} \right)$$

(16)

Apparently, the control performance is merely determined by the value of parameter T_0. In the practice of navigation, the wave action is a high-frequency disturbance for the ship and its frequency spectrum lies in the range of 0.3–1.25 rad/s. If the value of parameter T_0 is appropriately selected, the wave frequency spectrum of the ship can be neglected. Usually, its values lie outside the range 0.8–3.3. When the ship type or tonnage of the tanker changes, the value of the parameter T_0 can be properly re-selected to obtain the appropriate controller.

5.2 The verification of stabilization effectiveness

The unstable plant $G(s)$ in Equation (10) can be mirror-mapped into its corresponding minimum phase plant $G_m(s)$ based on the MMT, as shown in Equation (17).

$$G_m(s) = \frac{0.019}{s(153.7s+1)}$$

(17)
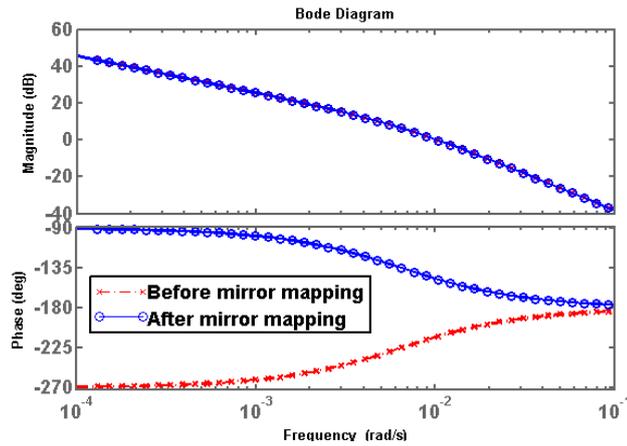
Fig. 3 Bode diagram of $G(s)$ and $G_m(s)$ before and after mirror mapping

From the Bode diagrams of unstable and stable plants shown in Figure 3, the spectrums are obviously similar. Then, the controller $C_m(s)$ is designed on the basis of the stable plant $G_m(s)$ given by Equation (18) wherein $T_0 = 4$ s. Moreover, the controller $C(s)$ is designed based on the unstable plant $G(s)$ given by Equation (19) for verifying the stabilization.

$$C_m(s) = \frac{1}{4s+2} \cdot \left(\frac{153.7s}{0.076} + \frac{1}{0.076} \right)$$

(18)

$$C(s) = \frac{1}{4s+2} \cdot \left(\frac{153.7s}{0.076} - \frac{1}{0.076} \right)$$

(19)

According to CGSA, the controller $C_m(s)$ designed on the basis of the stable plant $G_m(s)$ can stabilize the unstable plant $G(s)$. The simulation experiment is performed to testify the conclusion, and the results are as shown in Figures 4 and 5. It is obvious that the unstable plant $G(s)$ is successfully and perfectly stabilized using the controller $C_m(s)$. According to the Nyquist stability criterion, if the open-loop system is unstable and has an unstable pole, the closed-loop system is stable if and only if the Nyquist curve of the open-loop system encircles

the point (-1, $j0$) once in the counter-clockwise direction. Figure 6 shows the Nyquist curve of the open-loop system $G(s)$ $Cm(s)$ of the directionally unstable large tanker. Note that the curve satisfies the Nyquist stability criterion. Then, the controller designed is utilized to control the yaw motion of the large tanker. However, the unstable plant $G(s)$ is stabilized by the controller $C(s)$. Nevertheless, the stabilization of the controller $C(s)$ is caused by the zero pole cancellation, in which the zero point of the controller $C(s)$ is cancelled by the pole of the unstable plant $G(s)$. The zero pole cancellation will be described further in Section 6.1.
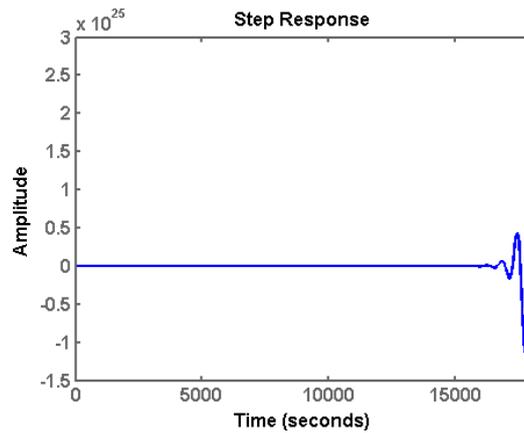
Fig. 4 Closed-loop step response of an unstable plant $G(s)$ without control

(a)   (b)
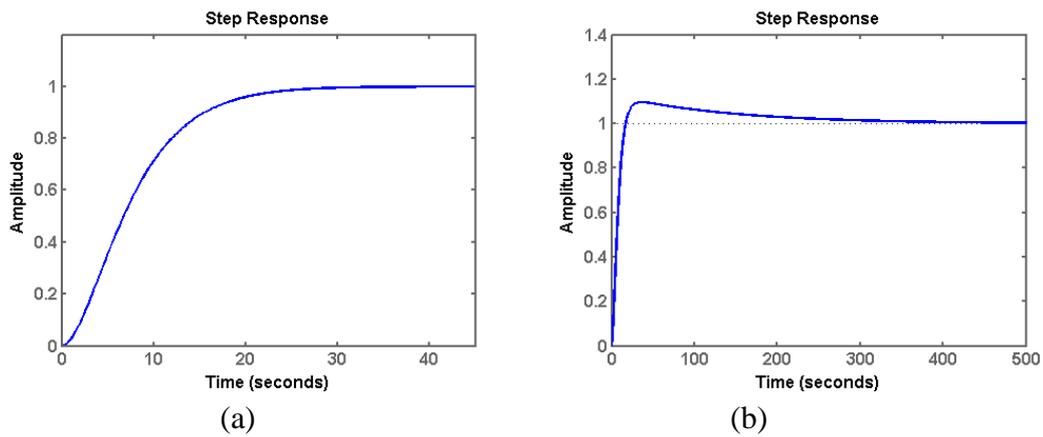
Fig. 5 Closed-loop step response of the unstable plant under control of $C(s)$ (a) and $C_m(s)$ (b)

Fig. 6 Nyquist curve of the open-loop system $G(s)C_m(s)$

Bai Chunjiang, Wang Hui, Ju Tingting
Shi Hanwen
Course-keeping control for directionally unstable
large tankers using the mirror-mapping technique
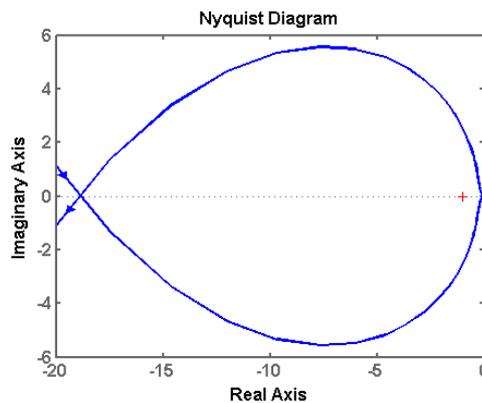
6. Numerical simulations and analysis of the results

6.1 Control performance for Nominal model

MATLAB is utilized to simulate the course-keeping control of a 389, 100 ton large tanker. To be more consistent with the motion characteristics of the ship, the third order Nomoto model in Equation (8) is consequently selected as the controlled plant in this note. The numerical simulation results of the nominal model are shown in Figures 7 and 8, without considering the influence of external wind and wave disturbances acting on the ship; however, this is accomplished with the steering gear characteristics for safety consideration in a manner such that the maximum rudder angle saturation limit is set to $\pm 30°$. From the simulation results, the directionally unstable large tanker under control of controller $C_m(s)$ can quickly and smoothly track the course, and not show any steady-state errors in the whole process, which indicates that the controller has a good dynamic and steady-state performance.

(a) (b)
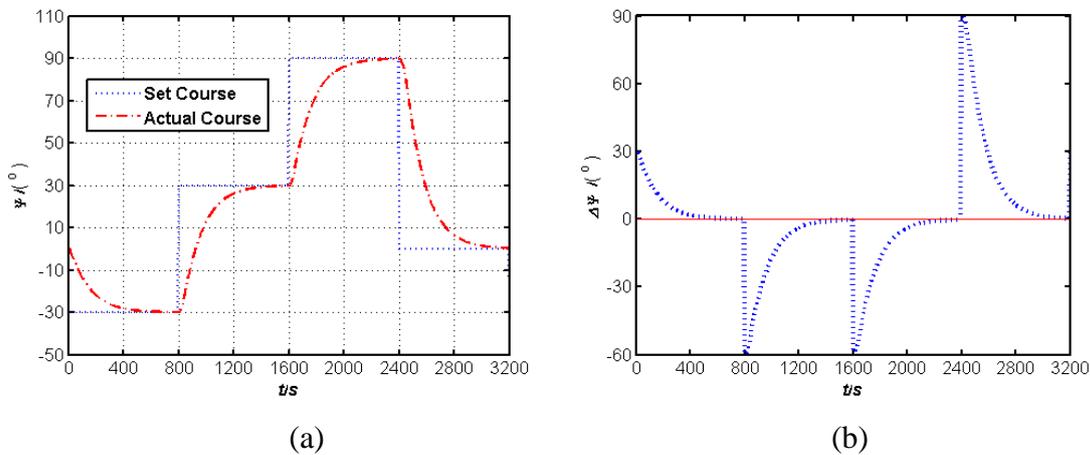
Fig. 7 Nominal model simulation result of course ψ (a) and course deviation $\triangle\psi$ (b).
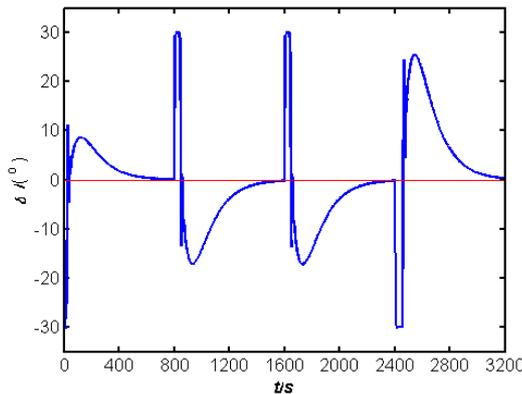
Fig. 8 Nominal model simulation result of rudder angle δ

Furthermore, the numerical simulation of unstable plant $G(s)$ in Equation (10) and controller $C(s)$ is conducted under identical conditions. The simulation results are shown in Figure 9. Clearly, the controller $C(s)$ cannot control the ship to track the set course; therefore, the controller $C(s)$ cannot be utilized to stabilize the directionally unstable large tanker for the nonlinearity of the steering gear, which prevents the zero pole cancellation mentioned in Section 5.2. The MMT should be adopted in the design process proposed in this note, which is a crucial and extremely effective technique.
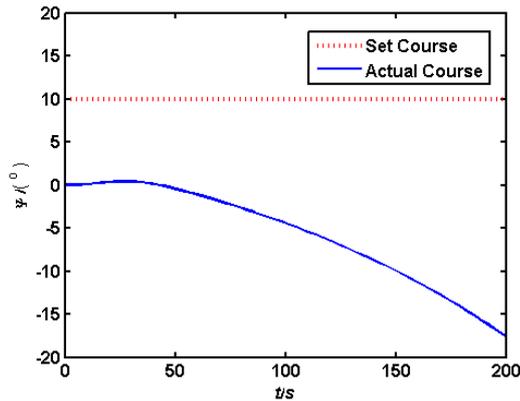
Fig. 9. Nominal model simulation result of course ψ for G(s) and C(s)

6.2   Control performance for Perturbed model

To be consistent with the practice of navigation, the external wind and wave disturbances acted on the ship is considered in the perturbed model. The second order wave transfer function, shown in Equation (20), corresponding to Beaufort No. 6 driven by white noise, is utilized to describe the wave disturbance, which is approved by the International Towing Tank Conference (ITTC). The Gaussian white noise is adopted to describe the wind disturbance. Figure 10 shows that subsequent to considering the wind and wave disturbances, the numerical simulation results of the ship heading angle ψ and the rudder angle δ.

$$h(s) = \frac{0.4198s}{s^2 + 0.3638s + 0.3675} \qquad (20)$$

(a)

(b)
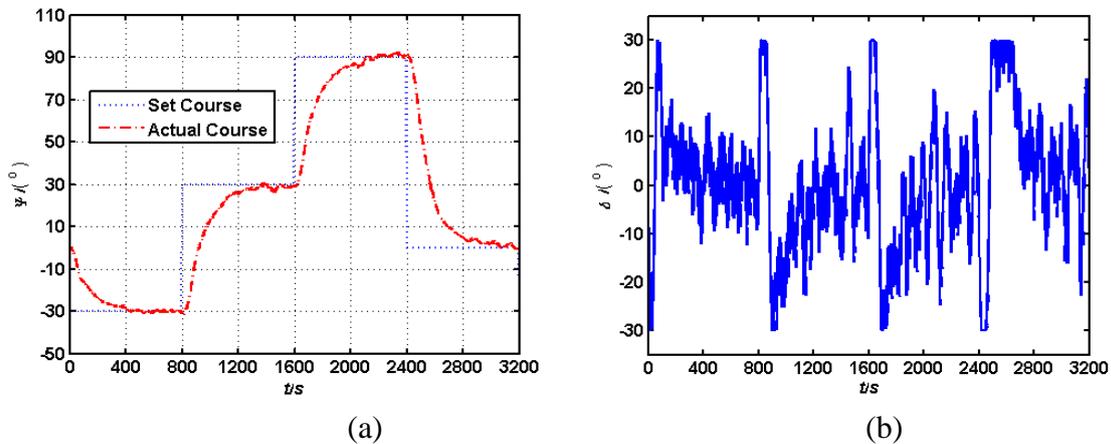
Fig.10 Perturbed model simulation result of course ψ (a) and rudder angle δ (b)

The simulation results show that the course keeping controller designed here for the perturbed model of the directionally unstable large tanker can quickly control the ship to track the set course. The rudder angle applied is consistent with the practice of navigation, i.e., large rudder angles ±30° for fast tracking the set course in the initial stage of the course changing and small rudder angles less than ±10° to alleviate the external wind and wave disturbances acting on the ship in the final stage of the course keeping. The controller designed on the basis of the second order Nomoto model can still quickly track the set course for the perturbed model, thus showing good dynamic performance. Furthermore, there is no excessive overshoot in the whole course keeping process, which reflects good steady-state performance of the controller.

Furthermore, the simulation results are satisfactory when the characteristics of the steering gear and the external wind and wave disturbances are not considered in the design of

the controller; however, these factors are considered in the simulation, which is equivalent to the model perturbation, indicates that the controller has good robust performance. Moreover, the controller designed is structurally equivalent to a LPD plus the first-order filter controller that allows for easy for engineering implementation. Thus, this controller has satisfactory control performance and strong robustness and meets the requirements of navigation practice.

7. Conclusions

In this study, we presented a concise controller design process for the course-keeping control of directionally unstable large tankers based on MMT and CGSA. We specifically focused on the pole in the right half plane of the unstable plant. The successful simulation results show that the controller designed through the proposed control process can stabilize the unstable plant of course unstable ship, particularly large tankers. Under the general requirements of control engineering and navigation practice, the controller has shown good control performance and strong robustness, as well as provided appropriate rudder angle output that meets the requirements of navigation operation practice. The proposed control scheme has the advantages of concise form and a simple and fast parameter-tuning procedure, thus allowing easy implementation in practice and more flexibility in application to other unstable plants of large tankers. Furthermore, this study has important reference value for practical application to guarantee the navigation safety of large tankers. However, instability phenomena may exist in other directions, e.g., roll motion; future work will focus on this area.

Acknowledgements

REFERENCES

[1]   G. Stein, "Respect the unstable," *Control Systems, IEEE,* vol. 23, pp. 12-25, 09/01 2003, doi: https://doi.org/10.1109/MCS.2003.1213600

[2]   T. Fossen, *Handbook of Marine Craft Hydrodynamics and Motion Control*. 2011. https://doi.org/10.1002/9781119994138

[3]   K. Spyrou and J. Thompson, "The nonlinear dynamics of ship motions: A field overview and some recent developments," *Philosophical Transactions of The Royal Society A Mathematical Physical and Engineering Sciences,* vol. 358, pp. 1735-1760, 06/15 2000, doi: https://doi.org/10.1098/rsta.2000.0613

[4]   I. Bačkalov *et al.*, "Ship stability, dynamics and safety: Status and perspectives from a review of recent STAB conferences and ISSW events," *Ocean Engineering,* vol. 116, pp. 312-349, 04/01 2016, doi: https://doi.org/10.1098/rsta.2000.0613

[5]   T. Manderbacka *et al.*, "An overview of the current research on stability of ships and ocean vehicles: The STAB2018 perspective," *Ocean Engineering,* vol. 186, p. 106090, 2019/08/15/ 2019, doi: https://doi.org/10.1016/j.oceaneng.2019.05.072

[6]   H. Yasukawa, "Maneuvering hydrodynamic derivatives and course stability of a ship close to a bank," *Ocean Engineering,* vol. 188, p. 106149, 09/01 2019, doi: https://doi.org/10.1016/j.oceaneng.2019.106149

[7]   A. Fitriadhy, *Course Stability of a Ship Towing System in Wind*. 2015.

[8]   M. Angelou and K. Spyrou, *Modeling sailing yachts' course instabilities considering sail shape deformations*. 2015.

[9]   S. Sutulo and C. Guedes Soares, "Numerical study of some properties of generic mathematical models of directionally unstable ships," *Ocean Engineering - OCEAN ENG,* vol. 32, 11/12 2004, doi: https://doi.org/10.1016/j.oceaneng.2004.05.008

[10]   Kim D., Kim SH., Han JS., Kim SJ., Paik KJ., " A STUDY ON THE SENSITIVITY ANALYSIS OF THE HYDRODYNAMIC DERIVATIVES ON THE MANEUVERABILITY OF KVLCC2 IN

SHALLOW WATER," BRODOGRADNJA /Shipbuilding, vol. 68, no. 4, pp. 1-12, 2017, doi: https://doi.org/10.21278/brod68401

[11] Dlabac T., Calasan M., Krcum M., Marvucic N., " PSO-BASED PID CONTROLLER DESIGN FOR SHIP COURSE-KEEPING AUTOPILOT, " BRODOGRADNJA /Shipbuilding, vol. 70, no. 4, pp. 1-15, 2019, doi: https://doi.org/10.21278/brod70401

[12] Demirel H., Balin A., Çelik E., Alarçin F., " A FUZZY AHP AND ELECTRE METHOD FOR SELECTING STABILIZING DEVICE IN SHIP INDUSTRY, " BRODOGRADNJA /Shipbuilding, vol. 69, no. 3, pp. 61-77, 2018, doi: https://doi.org/10.21278/brod69304

[13] Guoqing Zhang, Chenliang Zhang, Jiqiang Li, Xianku Zhang. Improved composite learning path-following control for the underactuated cable-laying ship via the double layers logical guidance, Ocean Engineering, 2020, 207: 107342. https://doi.org/10.1016/j.oceaneng.2020.107342

[14] Guoqing Zhang, Mingqi Yao, Junhao Xu, Weidong Zhang. Robust neural event-triggered control for dynamic positioning ships with actuator faults, Ocean Engineering, 2020, 207: 107292. https://doi.org/10.1016/j.oceaneng.2020.107292

[15] Guoqing Zhang, Shengjia Chu, Xu Jin, Weidong Zhang. Composite neural learning fault-tolerant control for underactuated vehicles with event-triggered input, IEEE Transactions on Cybernetics, 10.1109/TCYB.2020.3005800, 2020. https://doi.org/10.1109/TCYB.2020.3005800

[16] Guan wei,zhou ht, su zj,zhang xk,zhao c, Ship steering control based on quantum neural network, complexity, 2019(5) https://doi.org/10.1155/2019/3821048

[17] D. Neuffer and D. Owens, "Global stabilization of unstable ship dynamics using PD control," 01/01 1991, doi: 10.1109/CDC.1991.261359. https://doi.org/10.1109/CDC.1991.261359

[18] W. Gierusz, "Simulation Model of the Shiphandling Training Boat "Blue Lady"," *IFAC Proceedings Volumes,* vol. 34, no. 7, pp. 255-260, 2001/07/01/ 2001, doi: https://doi.org/10.1016/S1474-6670(17)35092-9

[19] M. L. P. J. R. Andrzej, "DESIGN OF THE SHIP COURSE CONTROL SYSTEM," presented at the INTERNATIONAL DESIGN CONFERENCE - DESIGN 2006 Dubrovnik, 2006.

[20] Z. Gang, Q. H. Yao, Y. B. Chen, Y. Y. Zhou, and L. WenKui, "A Study of Stability of Straight-line Tracking Control System for Underactuated Ship," *Acta Automatica Sinica,* vol. 33, no. 4, pp. 378-384, 2007.

[21] L. P. Perera and C. G. Soares, "Sliding Mode Controls in Partial Feedback Linearization applied to Unstable Ship Steering," *IFAC Proceedings Volumes,* vol. 45, no. 27, pp. 459-464, 2012/01/01/ 2012, doi: https://doi.org/10.3182/20120919-3-IT-2046.00078

[22] L. Perera and C. Guedes Soares, "Pre-filtered sliding mode control for nonlinear ship steering associated with disturbances," *Ocean Engineering,* vol. 51, pp. 49-62, 09/01 2012, doi: https://doi.org/10.1016/j.oceaneng.2012.04.014

[23] M. A. Abkowitz, "Lectures on ship hydrodynamics-steering and manoeuvrability," 1964.

[24] C. Å. Källström, Karl Johan LU ; Byström, L. and Norrbin, N. H., "Further Studies of Parameter Identification of Linear and Nonlinear Ship Steering Dynamics," Department of Automatic Control, 1977.

[25] X. Zhang and G. Zhang, "Stabilization of pure unstable delay systems by the mirror mapping technique," *Journal of Process Control,* vol. 23, pp. 1465–1470, 11/01 2013, doi: https://doi.org/10.1016/j.jprocont.2013.09.021

[26] Z. Su, X. Zhang, and X. Han, "Multitechnique Concise Robust Control for the Insulation Containment Space Pressure Control of LNG Carrier," *Mathematical Problems in Engineering,* vol. 2020, pp. 1-8, 02/08 2020, doi: https://doi.org/10.1155/2020/5759067

[27] J. Cao, X. Zhang, G. Yang, and X. Zou, "Robust Control of Pressure for LNG Carrier Cargo Handling System via Mirror-Mapping Approach," *Complexity,* vol. 2018, pp. 1-11, 2018. https://doi.org/10.1155/2018/7465391

[28] H. Zhao, X. Zhang, and X. Han, "Nonlinear control algorithms for efficiency-improved course keeping of large tankers under heavy sea state conditions," *Ocean Engineering,* vol. 189, p. 106371, 10/01 2019, doi: https://doi.org/10.1016/j.oceaneng.2019.106371

[29] X. Zhang and G. Zhang, "Novel robust control design for unstable systems with dual pole and dual zero," *Control & Cybernetics,* vol. 42, 2013.

[30]   G. Zhang, X. Zhang, and W. Guan, "Stability analysis and design of integrating unstable delay processes using the mirror-mapping technique," *Journal of Process Control,* vol. 24, pp. 1038–1045, 07/01 2014, doi: https://doi.org/10.1016/j.jprocont.2014.05.004

[31]   G. Zhang, X. Zhang, and W. Zhang, "Robust controller synthesis for high order unstable processes with time delay using mirror mapping technique," *Isa Transactions,* vol. 59, pp. 10-19, 2015, doi: https://doi.org/10.1016/j.isatra.2015.08.004

[32]   G. Zhang, B. Tian, W. Zhang, and X. Zhang, "Optimized robust control for industrial unstable process via the mirror-mapping method," *ISA Transactions,* vol. 86, pp. 9-17, 2019/03/01/ 2019, doi: https://doi.org/10.1016/j.isatra.2018.10.040.

[33]   X. x. WU, G. q. ZHANG, and W. d. ZHANG, "H∞ optimized control for pressure maintenance system of LNG tank via the mirror-mapping technique," *Control and Decision,* vol. 35, no. 2, pp. 501-506, 2020, doi: 10.13195/j.kzyjc.2018.0662.

Bai Chunjiang, baichunjiang@dlmu.edu.cn
Wang Hui*, wanghui2314@dlmu.edu.cn
Ju Tingting, bnutingting@163.com
Shi Hanwen, 18004265595@163.com
Navigation College, Dalian Maritime University, Dalian 116026, China